



Published in final edited form as:

*Environ Mol Mutagen.* 2013 October ; 54(8): 629–637. doi:10.1002/em.21795.

## Pyruvate Remediation of Cell Stress and Genotoxicity Induced by Haloacetic Acid Drinking Water Disinfection By-Products

Azra Dad<sup>1,2</sup>, Clara H. Jeong<sup>1</sup>, Justin A. Pals<sup>1</sup>, Elizabeth D. Wagner<sup>1,3</sup>, and Michael J. Plewa<sup>1,3,\*</sup>

<sup>1</sup>Department of Crop Sciences, University of Illinois at Urbana-Champaign, Urbana, Illinois

<sup>2</sup>Comsats Institute of Information Technology, Islamabad, Pakistan

<sup>3</sup>Safe Global Water Institute and NSF Science and Technology, Center of Advanced Materials for the Purification of Water with Systems, University of Illinois at Urbana-Champaign, Urbana, Illinois

### Abstract

Monohaloacetic acids (monoHAAs) are a major class of drinking water disinfection by-products (DBPs) and are cytotoxic, genotoxic, mutagenic, and teratogenic. We propose a model of toxic action based on monoHAA-mediated inhibition of glyceraldehyde-3-phosphate dehydrogenase (GAPDH) as a target cytosolic enzyme. This model predicts that GAPDH inhibition by the monoHAAs will lead to a severe reduction of cellular ATP levels and repress the generation of pyruvate. A loss of pyruvate will lead to mitochondrial stress and genomic DNA damage. We found a concentration-dependent reduction of ATP in Chinese hamster ovary cells after monoHAA treatment. ATP reduction per pmol monoHAA followed the pattern of iodoacetic acid (IAA) > bromoacetic acid (BAA) >> chloroacetic acid (CAA), which is the pattern of potency observed with many toxicological endpoints. Exogenous supplementation with pyruvate enhanced ATP levels and attenuated monoHAA-induced genomic DNA damage as measured with single cell gel electrophoresis. These data were highly correlated with the  $S_N2$  alkylating potentials of the monoHAAs and with the induction of toxicity. The results from this study strongly support the hypothesis that GAPDH inhibition and the possible subsequent generation of reactive oxygen species is linked with the cytotoxicity, genotoxicity, teratogenicity, and neurotoxicity of these DBPs.

### Keywords

DBP; GAPDH; SCGE; reactive oxygen species; monohaloacetic acids

---

© 2013 Wiley Periodicals, Inc.

\*Correspondence to: Michael J. Plewa, 364 NSRL, University of Illinois at Urbana-Champaign, 1101 W. Peabody Dr., Urbana, IL 61801, USA. mplewa@illinois.edu.

### AUTHOR CONTRIBUTIONS

Drs. Plewa and Wagner designed the study, conducted the statistical analyses of the data and provided overall study management. Ms. Dad conducted the experiments with the assistance of Ms. Jeong. Ms. Jeong and Ms. Dad conducted the mathematical analyses of the ATP and protein data. Mr. Pals conducted the literature review and participated in the development and evaluation of the experimental designs. Dr. Plewa and Ms. Dad prepared the manuscript draft with important intellectual input from Dr. Wagner, Ms. Jeong and Mr. Pals. All authors approved the final manuscript.

## INTRODUCTION

A preeminent public health accomplishment achieved during the last century was the disinfection of drinking water. Water treatment and distribution of disinfected water was an effective strategy in controlling waterborne diseases such as cholera, typhoid and dysentery [Cutler and Miller, 2005]. However, disinfection by-products (DBPs) are inadvertently generated when chlorine or other disinfectants react with organic matter present in source water [Cutler and Miller, 2005; Richardson, 2011]. Many DBPs are cytotoxic, genotoxic, mutagenic, carcinogenic and teratogenic [Richardson et al., 2007]. Epidemiological studies demonstrated an association between lifetime exposures to DBPs and increased risk of bladder cancer [Villanueva et al., 2004, 2007; Costet et al., 2011; Kogevinas, 2011], colorectal cancer [King et al., 2000; Rahman et al., 2010] and skin cancer [Karagas et al., 2008]. The U.S. Environmental Protection Agency (U.S. EPA) estimated that between 2 and 17% of bladder cancer cases in the United States may be induced by DBPs [U.S. Environmental Protection Agency, 1998]. Epidemiological studies also demonstrated an association between disinfected drinking water and adverse pregnancy outcomes [Costet et al., 2012; Jeong et al., 2012; Righi et al., 2012].

Currently, over 600 DBPs have been identified and the spectrum of DBP chemical classes are influenced by the source water, water contaminants and the disinfectant used [Zhang et al., 2000; Hua and Reckhow, 2007; Richardson, 2011]. In chlorinated water, the second largest occurring DBP chemical class is the haloacetic acids (HAAs) [Krasner et al., 2006]. The HAAs are the most highly regulated DBPs. The U.S. EPA regulates chloroacetic acid (CAA), dichloroacetic acid, trichloroacetic acid, bromoacetic acid (BAA), and dibromoacetic acid to a total maximum contaminant level of 60 µg/L [U.S. Environmental Protection Agency, 2006]. At all water sites measured, the U.S. EPA Information Collection Rule recorded the mean and 90th percentile concentration for the five regulated HAAs (HAA5) as 23 µg/L and 47.5 µg/L, respectively [McGuire et al., 2002].

HAAs are alkylating agents and follow  $S_N2$  reactivity, which is primarily dependent on the carbon-halogen bond length and the bond dissociation energy. The  $\alpha$ -carbon-halide ( $\alpha$ C-X) bond length follows the pattern of C-I > C-Br > C-Cl, which implies that the greater the bond length, the lower the dissociation energy required to react with the target molecule [Plewa et al., 2004]. Cytotoxic and genotoxic potencies induced by the monohaloacetic acids (monoHAAs) expressed the pattern of iodoacetic acid (IAA) > BAA >> CAA, which highly correlated to the  $S_N2$  reactivity,  $\alpha$ C-X bond length and  $\alpha$ C-X dissociation energy [Plewa et al., 2004].

HAAs are mutagenic in *Salmonella typhimurium* and Chinese hamster ovary (CHO) cells [Kargalioglu et al., 2002; Plewa et al., 2004; Zhang et al., 2010]. They are cytotoxic and genotoxic in CHO cells [Plewa et al., 2010], nontransformed human cells [Attene-Ramos et al., 2010] and toxic in a variety of other bioassays [Richardson et al., 2007]. The monoHAAs modulated the gene expression pathways of ATM, MAPK, p53, BRCA1, BRCA2, and ATR, in nontransformed human FHs 74-Int cells; these pathways are involved in stress response to DNA damage and regulate different stages in cell cycle progression or apoptosis [Attene-Ramos et al., 2010; Muellner et al., 2010]. FHs 74-Int cells originated

from a female fetus 3–4 months into gestation [Smith, 1979]. Recently, IAA induced malignant transformation in NIH/3T3 mouse embryonic fibroblast cells that progressed to highly aggressive fibrosarcomas when implanted in Balb/c nude mice [Wei et al., in press]. Under *ex-vivo* conditions, monoHAAs were teratogenic and induced dysmorphogenesis in three to six somite staged CD-1 mouse embryos and affected neural tube development, eye development and produced hypoplastic pharyngeal arches and anomalies in heart development [Hunter et al., 1996]. F344 rats gavaged with a mixture of HAA5 during gestation resulted in pregnancy loss and eye malformation in surviving litters [Narotsky et al., 2011].

IAA induced toxicity in hippocampal neuronal cells by inhibiting the glycolytic enzyme glyceraldehyde-3-phosphate dehydrogenase (GAPDH), which led to hypoglycemia and the generation of reactive oxygen species (ROS) [Hernandez-Fonseca et al., 2008]. Similar effects were induced by IAA in hippocampal astrocytes [Kahlert and Reiser, 2000]. The direct role of monoHAA-mediated inhibition kinetics of GAPDH and their high correlation with many toxicity measurements was recently published by our laboratory [Pals et al., 2011].

Our working hypothesis is that GAPDH is inhibited by monoHAAs, which reduces the generation of pyruvate and ATP that is required for the tricarboxylic acid (TCA) cycle for the further production of ATP. We postulate that the unavailability of pyruvate causes mitochondrial stress leading to the generation of ROS and a reduction in cellular ATP levels, which may lead to cytotoxicity. We also contend that increased levels of ROS induce genomic DNA damage in HAA-treated cells. If this hypothesis is correct, then supplementing monoHAA-treated cells with exogenous pyruvate should restore cellular ATP levels and prevent or reduce genomic DNA damage. The objective of this research was to test the first part of this hypothesis involving the impact of the monoHAAs on ATP levels and generation of pyruvate. We measured the impact of the monoHAAs on ATP levels and the induction of genomic DNA damage with and without pyruvate supplementation.

## MATERIALS AND METHODS

### Reagents

General reagents were purchased from Fisher Scientific (Itasca, IL) and Sigma Chemical (St. Louis, MO). The sources and purities of the monoHAAs used in this research are listed in Table I. Cell culture F12 medium and fetal bovine serum (FBS) were purchased from Fisher Scientific, and pyruvic acid was purchased from Acros Organics (NJ). Cell Titer-Glo reagent was purchased from Promega (Madison, WI). The monoHAAs were dissolved in dimethylsulfoxide (DMSO) and stored at  $-20^{\circ}\text{C}$  in sealed sterile glass vials (Supelco, Bellefonte, PA). Pyruvate was dissolved directly either in F12 or Hank's balanced salt solution (HBSS) according to the experimental design, while individual IAA, BAA and CAA stock solutions in DMSO (1 M) were diluted in F12 medium or HBSS depending upon the experimental design.

### Chinese Hamster Ovary Cells

CHO cell clone 11-4-8 was used [Wagner et al., 1998]. Cells were grown in 100 mm glass petri plates with F12 medium containing 5% FBS, 1% glutamine and 1% antibiotic-antimycotic solution at 37 °C in a humidified atmosphere of 5% CO<sub>2</sub>.

### ATP Analysis

Cellular ATP levels were determined after exposure to monoHAAs alone, pyruvic acid alone or monoHAAs plus pyruvic acid with a TUNE-SpectraMax Paradigm® Multi-Mode Microplate Detection Platform using Promega Cell Titer-Glo ATP reagents. The day before ATP analysis,  $3 \times 10^4$  CHO cells/well were cultured in a 96-well opaque microplate in 200 µL of F12 plus 5% FBS. The next day, the cells were washed with 100 µL of HBSS and treated with concentrations of the monoHAAs with and without pyruvic acid in 50 µL HBSS (with 1.3 mM CaCl<sub>2</sub> and 1.1 mM MgSO<sub>4</sub>). The microplate was covered with AlumnaSeal and incubated for 4 hr at 37 °C, 5% CO<sub>2</sub>. Each experiment contained a concurrent negative control, a bioluminescence background control, pyruvic acid (10 mM), the monoHAAs, monoHAAs plus pyruvic acid and an ATP standard curve. After a 4-hr incubation, the cells were washed with 100 µL of HBSS and supplemented with 10 mM pyruvate (for the pyruvate containing treatment groups), covered with AlumnaSeal and incubated for 30 min at 37 °C, 5% CO<sub>2</sub> and then equilibrated to room temperature for 30 min. The ATP contents of the cells were measured according to the manufacturer's protocol using 50 µL of Cell Titer-Glo ATP reagents. Data were collected in an Excel spreadsheet and used in calculating pmols of ATP.

### Protein Determination

Parallel ATP and protein analyses were performed. The day before the experiment,  $3 \times 10^4$  CHO cells/well were cultured in a 96-well flat bottom clear microplate in 200 µL of F12 plus 5% FBS. The next day, cells were treated with the monoHAAs with and without pyruvate as discussed above for the ATP analysis. After treatment, the cells were lysed by adding 25 µL of Solulyse® cell homogenizing solution (Genlantis, San Diego, CA). The microplate was covered with sterile AlumnaSeal and put on a rocker platform (at 37 °C) shaken for 5 min after which the plate was rotated and shaken for an additional 5 min. After cell lyses, 10 µL of the lysate from each well was transferred into a new microplate; into each well was added 10 µL of an anti-foaming agent (Sigma 204, 0.01% v/v), 40 µL of Bradford solution (BioRad), and 140 µL of dH<sub>2</sub>O for a final volume of 200 µL. A BioRad protein (BSA) standard was prepared on the same microplate, using 0.68 µg/µL of a BSA standard solution. The contents of each well were carefully mixed and incubated at room temperature for 20 min. The absorbance was read at 595 nm using a SpectraMax Molecular Device plate reader. The data were collected in an Excel spreadsheet and the mg of protein was calculated for each well.

### Single Cell Gel Electrophoresis Assay

The alkaline single cell gel electrophoresis (SCGE) or Comet assay is a sensitive, quantitative method for the detection of genomic DNA damage in individual cells [Tice et al., 2000; Rundell et al., 2003]. CHO cells were treated with a series of concentrations of

IAA, BAA or CAA with and without pyruvic acid and the level of genomic DNA damage was measured. The SCGE microplate assay was performed as described by [Wagner and Plewa, 2009]. The day before treatment,  $4 \times 10^4$  cells were cultured into each well of a 96-well microplate in 200  $\mu$ L of F12 plus 5% FBS and incubated overnight. The following day, cells were washed twice with 100  $\mu$ L of HBSS and treated with a series of concentrations of a monoHAA alone, pyruvic acid alone, and the monoHAA plus pyruvic acid in a total volume of 25  $\mu$ L. The cells were covered with sterile AlumnaSeal and incubated for 4 hr at 37 °C in a humidified atmosphere of 5% CO<sub>2</sub>. Each experiment had a concurrent negative control (F12 medium only) and a positive control (3.8 mM ethylmethanesulfonate). After treatment, the cells were washed with HBSS, harvested with a 0.05% trypsin +53  $\mu$ M EDTA solution and incorporated into agarose microgels. For each concentration group, acute cytotoxicity was measured using the vital dye trypan blue [Phillips, 1973]. The microgels were electrophoresed and analyzed if the viability of the cell suspensions was >70%. The microgels were placed in lysing solution overnight at 4 °C to remove cell membranes (2.5 M NaCl, 100 mM Na<sub>2</sub>EDTA, 10 mM Trizma base, 26 g of NaOH and 1% sodium lauryl sarcosinate, pH 10) with 10% DMSO and 1% Triton X-100 added just prior to use. The microgels were rinsed twice with cold deionized water and the DNA was denatured for 20 min in electrophoresis buffer (1 mM Na<sub>2</sub>EDTA and 300 mM NaOH, pH 13.5). The microgels were electrophoresed for 40 min at 25 V, 300 mA (0.72 V/cm) at 4 °C. After electrophoreses, the microgels were neutralized with 400 mM Tris buffer (pH 7.5), dehydrated in methanol (4 °C) and dried for 5 min at 50 °C. The microgels were stored in the dark at room temperature. To analyze the microgels, they were first hydrated in deionized water for 30 min at 4 °C, stained with 65  $\mu$ L of 20  $\mu$ g/mL ethidium bromide and rinsed in cold deionized water. After staining, a cover slip was applied onto the microgel and 25 randomly selected nuclei per microgel were analyzed under a Zeiss fluorescence microscope with the Comet IV imaging system (Perspective Instruments, Suffolk, UK). The data were automatically transferred to an Excel spreadsheet. For DNA damage the unit of measure for each microgel was the average % tail DNA, which is the amount of DNA that migrated into the gel from the nucleus. The mean % tail DNA values were calculated for the microgels in a treatment group and were analyzed with an ANOVA statistical test. If a significant *F* value of  $P < 0.05$  was obtained, a Holm-Sidak pairwise comparison versus the control group analysis was conducted (power = 0.8 at  $\alpha = 0.05$ ).

## RESULTS AND DISCUSSION

Five HAAs are regulated by the U.S. EPA; two of the five are BAA and CAA [U.S. Environmental Protection Agency, 2006]. MonoHAAs are cytotoxic, genotoxic, mutagenic, and teratogenic [Richardson et al., 2007]. This study extends our research on the molecular mechanism(s) of toxicity of these important DBPs by investigating the impact of monoHAAs on cellular ATP levels, their induction of genomic DNA damage and the attenuation of this DNA damage by pyruvate supplementation.

Previous studies demonstrated that IAA blocked glycolysis by inhibiting GAPDH that led to neurotoxicity [Matthews et al., 1997; Kahlert and Reiser, 2000; Hernandez-Fonseca et al., 2008], ROS generation [Matthews et al., 1997; Hernandez-Fonseca et al., 2008], ATP depletion [Kahlert and Reiser, 2000; Hernandez-Fonseca et al., 2008] and disruption of

intracellular  $\text{Ca}^{2+}$  homeostasis [Kahlert and Reiser, 2000; Chinopoulos and Adam-Vizi, 2006]. We recently demonstrated that the relative rates of monoHAA-induced GAPDH inhibition kinetics were highly correlated with many toxicity metrics [Pals et al., 2011]. Central to its glycolytic function is a conserved cysteine residue in the active site of GAPDH. This cysteine serves as a nucleophile in the first catalytic step in the conversion of glyceraldehyde-3-phosphate to 1,3-bis-phosphoglycerate [Nakajima et al., 2007]. The  $\alpha$ -carbon of each monoHAA is a primary alkyl halide and an electrophile due to electron withdrawal from the carbon by the halogen substituent. IAA, BAA, and CAA inhibit GAPDH when the  $\alpha$ -carbon undergoes an  $\text{S}_{\text{N}}2$  reaction with the nucleophilic thiol group on the catalytic cysteine residue. This results in a carboxymethylated cysteine which irreversibly inhibits the catalytic function of the enzyme. Our overall working hypothesis is that the monoHAAs inhibit GAPDH by alkylating the thiol group at the GAPDH active site. This leads to glycolytic ATP depletion and blocks the production of pyruvate that is a mitochondrial substrate for the TCA cycle [Tristan et al., 2011]. Pyruvate starvation enhances mitochondrial stress, disrupts the TCA cycle and affects the generation of reducing power (NADH and  $\text{FADH}_2$ ) within mitochondria during the TCA cycle. This deficiency in reducing power disturbs normal oxidative phosphorylation, which eventually generates ROS, depletes mitochondrial ATP and increases cytosolic  $\text{Ca}^{2+}$  concentration [Nakajima et al., 2007; Hernandez-Fonseca et al., 2008; Csordas and Hajnoczky, 2009; Peng and Jou, 2010]. This proposed mechanism is supported in that IAA-induced mutagenicity in *Salmonella typhimurium* and genotoxicity in CHO cells was repressed by the antioxidants catalase and butylated hydroxyanisole [Cemeli et al., 2006]. We believe that ATP depletion and ROS generation are the principal forcing mechanisms for monoHAA-mediated toxicity [Schlisser et al., 2010; Pals et al., 2011].

### Depletion of ATP by MonoHAAs

MonoHAAs inhibited GAPDH kinetics with a rank order of  $\text{IAA} > \text{BAA} > \text{CAA}$  [Pals et al., 2011]. We proposed that cells exposed to monoHAAs would express ATP depletion. To test this, CHO cells were treated with 25 and 40  $\mu\text{M}$  IAA, 60  $\mu\text{M}$  BAA and 6 mM CAA for 4 hr in HBSS. The concentrations of each monoHAA were previously determined to be genotoxic in CHO cells without acute cytotoxicity [Komaki et al., 2009]. The cellular ATP levels (as the average bioluminescence unit) for monoHAA-treated cells were significantly reduced as compared to the negative control. The ATP levels with CAA-treated cells were approximately the same as the blank (Fig. 1). These data demonstrate that IAA, BAA and CAA significantly reduced cellular ATP levels; however, this experimental design could generate an artifact. Although, by observation, we did not detect CHO cell cytotoxicity after 4 hr, we did not have a direct quantitative measurement of cell viability of the cell suspensions from which these ATP measurements were generated.

### Pyruvate Supplementation and ATP Levels in monoHAA-Treated Cells

To avoid the artifacts that may be associated with the direct ATP measurements alone, the experimental designs were refined and expanded to include protein analyses. We determined the minimum concentration of each monoHAA in HBSS (with 1.3 mM  $\text{CaCl}_2$  and 1.1 mM  $\text{MgSO}_4$ ) that induced a significant reduction in cellular ATP levels. The lowest noncytotoxic concentrations of IAA, BAA and CAA that induced a significant reduction in ATP levels as



compared to each concurrent negative control was 3  $\mu$ M, 6  $\mu$ M, and 1 mM, respectively (Fig. 2). Using these concentrations of IAA, BAA and CAA, we conducted parallel experiments to determine the absolute amount of ATP and the total protein content of each cell suspension within each treatment group. Each monoHAA treatment had a negative control, a blank control, a pyruvate control, a monoHAA treatment and a monoHAA plus 10 mM pyruvate treatment. The number of replicate clones for the IAA treatment group was 40 while for BAA and CAA the number of replicate clones were 37 and 32, respectively. This experimental design allowed us to determine concentrations of ATP and protein for each CHO cell suspension for a precise measurement of ATP depletion and restoration. The concentration of ATP as pmol/mg protein for each monoHAA treatment group is presented in Table II. Figure 3 illustrates cellular ATP levels (pmol ATP/mg protein) normalized as 100% for each concurrent negative control for each monoHAA treatment group. A reduction in ATP levels was observed with exposures to 3  $\mu$ M IAA, 6  $\mu$ M BAA and 1 mM CAA with levels of 18.7, 48.2, and 50.8%, respectively, of the concurrent negative controls. When monoHAA-treated cells were simultaneously treated with 10 mM pyruvate a significant recovery of cellular ATP levels was measured. For IAA, ATP concentrations increased from 18.7 to 45.0% of the concurrent negative control. Similar responses were observed for BAA (48.2–122.1%) and CAA (50.8–80.2%) (Fig. 3). These data support our hypothesis that a major pathway in the toxic mode of action by the monoHAAs is the irreversible inhibition of GAPDH and the subsequent reduction of cellular ATP levels and a blockage in the generation of pyruvate from glucose.

From these ATP measurements, an interesting and familiar pattern of response emerged. Comparing the monoHAAs, the CHO cells treated with IAA expressed the greatest reduction in cellular ATP levels (0.54%) per pmol IAA as compared to the negative control. For the BAA and CAA treatment groups, the reduction in cellular ATP levels per pmol monoHAA was 0.15% for BAA and approximately 0.001% for CAA (Table II). The monoHAA-mediated ATP depletion followed a rank order of IAA > BAA > CAA. This pattern and magnitude of ATP depletion directly correlated with the  $\alpha$ C–X bond length and relative alkylation potential of each monoHAA and was inversely correlated with the  $\alpha$ C–X bond dissociation energy (Table III). ATP depletion was highly correlated with the inhibition kinetics of GAPDH [Pals et al., 2011] (Table IV). Of importance is that ATP depletion by the monoHAAs (Table II) are highly correlated with diverse measurements of toxicity including cytotoxicity, genotoxicity, mutagenicity and teratogenicity published in the literature over the past 17 years (Table IV).

### Pyruvate Attenuation of MonoHAA-Induced Genotoxicity

The monoHAAs are direct-acting mutagens in *S. typhimurium* [Kargalioglu et al., 2002; Plewa et al., 2004] and in CHO cells [Zhang et al., 2010] and do not require monooxygenase-mediated metabolic activation for genotoxicity in CHO cells [Plewa et al., 2010]. The monoHAAs do not induce genomic damage via direct alkylation of DNA [Pals et al., 2011]. We suggest that monoHAAs induce DNA damage by alkylating the thiol group of the cysteine residue in the active site of GAPDH [Jenkins and Tanner, 2006]. The resulting reduction in ATP and pyruvate levels leads to ROS generation [Matthews et al., 1997] and subsequent DNA damage [Kumagai et al., 2008]. We postulated that if genomic DNA

damage is linked to GAPDH inhibition then supplementing cells with exogenous pyruvate should lead to a reduction in genomic DNA damage. To test this hypothesis, CHO cells were treated with monoHAA concentrations that did not induce acute cytotoxicity but were strongly genotoxic in the SCGE assay (Table V). We treated CHO cells with 25  $\mu$ M IAA, 60  $\mu$ M BAA or 6 mM CAA for 4 hr with and without 10 mM pyruvate. Genomic DNA damage was measured by the SCGE assay. The mean % tail DNA values for the negative control and 10 mM pyruvate control were 2.80 and 2.79, respectively and were not statistically different (Table V). All of the monoHAAs induced a significant level of DNA damage in CHO cells as compared to the negative controls. However, when 25  $\mu$ M IAA was supplemented with pyruvate a significant reduction in the mean SCGE % tail DNA values was observed (IAA alone, 21.5 compared to IAA + pyruvate, 10.6). Similar reductions in genomic DNA damage with pyruvate supplementation were recorded for 60  $\mu$ M BAA (BAA alone and BAA + pyruvate, 49.8 and 8.1% tail DNA, respectively), and 6 mM CAA (CAA alone and CAA + pyruvate, 47.2 and 24.9% tail DNA, respectively) (Table V). When these data were normalized such that the concurrent monoHAA positive control equaled 100% of the observed DNA damage, pyruvate supplementation significantly repressed the induction of genomic DNA damage (Fig. 4).

This proposed model for the toxicity of the monoHAAs has a unifying pattern of response (IAA > BAA > CAA) that we identified a decade ago [Plewa et al., 2004]. Although many iodinated DBPs are more toxic than their brominated and chlorinated analogues [Plewa et al., 2008; Plewa and Wagner, 2009], the monoHAAs provide a class of substrates with a single variable (the single halogen atom bound to the  $\alpha$ -carbon). Originally we believed that the monoHAAs induced genomic damage via direct alkylation of DNA; there was a high correlation among the alkylating potential,  $\alpha$ C-X bond dissociation energy, cytotoxicity and genotoxicity in *S. typhimurium* and CHO cells (Table IV) [Plewa et al., 2004]. These DBPs are direct-acting mutagens in that they do not require S9 microsomal activation in *S. typhimurium* [Plewa et al., 2004] or CHO cells [Zhang et al., 2010]. However, we discovered that while the monoHAAs induce DNA damage using the cellular SCGE assay (treatment of intact cells), the capacity to damage DNA was lost when analyzed with the acellular SCGE assay (treatment of nuclei) [Pals et al., 2011]. We concluded that DNA was not the direct target of the monoHAAs. Previously CAA and IAA were demonstrated to inhibit GAPDH without affecting other glycolytic enzymes [Sakai et al., 2005; Hernandez-Fonseca et al., 2008]. The linkage between GAPDH inhibition and the quantitative toxicity of the monoHAAs was established by the inhibition kinetics of GAPDH, which also expressed the pattern of IAA > BAA > CAA. GAPDH inhibition kinetics were highly correlated with a host of toxicity metrics (Table IV) [Pals et al., 2011]. From this study, we further define the role of GAPDH inhibition and the induction of toxicity. Cellular ATP depletion in monoHAA-treated cells followed the pattern of IAA > BAA > CAA and was highly correlated with their  $S_N2$  alkylating potential and with the induction of toxicity (Table III). Pyruvate is a product of glycolysis; pyruvate supplementation restored ATP levels and reduced the genomic DNA damage in monoHAA-treated cells. These results strongly support our hypothesis that GAPDH inhibition and subsequent generation of ROS is linked with cytotoxicity, genotoxicity, teratogenicity, and neurotoxicity and may play a substantive role in neurodegenerative diseases such as Alzheimer's disease [Butterfield et



al., 2010]. The data presented here establish a comprehensive and testable model for the toxic mechanisms of the haloacetic acids, a major class of drinking water DBPs.

## Acknowledgments

Grant sponsor: Center of Advanced Materials for the Purification of Water with Systems (Water-CAMPWS, National Science Foundation Science and Technology Center); Grant number: CTS-0120978; Grant sponsor: U.S. EPA Star Grant; Grant number: R834867; Grant sponsor: NIEHS Predoctoral Fellowship; Grant number: T32 ES007326; Grant sponsor: Institute of Information Technology, Pakistan (Comsats Fellowship).

## REFERENCES

- Attene-Ramos MS, Wagner ED, Plewa MJ. Comparative human cell toxicogenomic analysis of monohaloacetic acid drinking water disinfection byproducts. *Environ Sci Technol.* 2010; 44:7206–7212. [PubMed: 20540539]
- Butterfield DA, Hardas SS, Lange MLB. Oxidatively modified glyceraldehyde-3-phosphate dehydrogenase (GAPDH) and Alzheimer's disease: Many pathways to neurodegeneration. *J Alzheimers Disease.* 2010; 20:369–393. [PubMed: 20164570]
- Cemeli E, Wagner ED, Anderson D, Richardson SD, Plewa MJ. Modulation of the cytotoxicity and genotoxicity of the drinking water disinfection byproduct iodoacetic acid by suppressors of oxidative stress. *Environ Sci Technol.* 2006; 40:1878–1883. [PubMed: 16570611]
- Chinopoulos C, Adam-Vizi V. Calcium, mitochondria and oxidative stress in neuronal pathology. Novel aspects of an enduring theme. *FEBS J.* 2006; 273:433–450. [PubMed: 16420469]
- Costet N, Villanueva CM, Jaakkola JJ, Kogevinas M, Cantor KP, King WD, Lynch CF, Nieuwenhuijsen MJ, Cordier S. Water disinfection by-products and bladder cancer: Is there a European specificity? A pooled and meta-analysis of European case-control studies. *Occup Environ Med.* 2011; 68:379–385. [PubMed: 21389011]
- Costet N, Garlandezec R, Monfort C, Rouget F, Gagniere B, Chevrier C, Cordier S. Environmental and urinary markers of prenatal exposure to drinking water disinfection by-products, fetal growth, and duration of gestation in the PELAGIE birth cohort (Brittany, France, 2002-2006). *Am J Epidemiol.* 2012; 175:263–275. [PubMed: 22156019]
- Csordas G, Hajnoczky G. SR/ER-mitochondrial local communication: Calcium and ROS. *Biochim Biophys Acta.* 2009; 1787:1352–1362. [PubMed: 19527680]
- Cutler D, Miller G. The role of public health improvements in health advances: The twentieth-century United States. *Demography.* 2005; 42:1–22. [PubMed: 15782893]
- Hernandez-Fonseca K, Cardenas-Rodriguez N, Pedraza-Chaverri J, Massieu L. Calcium-dependent production of reactive oxygen species is involved in neuronal damage induced during glycolysis inhibition in cultured hippocampal neurons. *J Neurosci Res.* 2008; 86:1768–1780. [PubMed: 18293416]
- Hua GH, Reckhow DA. Comparison of disinfection byproduct formation from chlorine and alternative disinfectants. *Water Res.* 2007; 41:1667–1678. [PubMed: 17360020]
- Hunter ES, Rogers EH, Schmid JE, Richard A. Comparative effects of haloacetic acids in whole embryo culture. *Teratology.* 1996; 54:57–64. [PubMed: 8948541]
- Jenkins JL, Tanner JJ. High-resolution structure of human D-glyceraldehyde-3-phosphate dehydrogenase. *Acta Cryst.* 2006; 62:290–301.
- Jeong CH, Wagner ED, Siebert VR, Anduri S, Richardson SD, Daiber EJ, McKague AB, Kogevinas M, Villanueva CM, Goslan EH, Luo W, Isabelle LM, Pankow JF, Grazuleviciene R, Cordier S, Edwards SC, Righi E, Nieuwenhuijsen MJ, Plewa MJ. The occurrence and toxicity of disinfection byproducts in European drinking waters in relation with the HIWATE epidemiology study. *Environ Sci Technol.* 2012; 46:12120–12128. [PubMed: 22958121]
- Kahlert S, Reiser G. Requirement of glycolytic and mitochondrial energy supply for loading of Ca<sup>(2+)</sup> stores and InsP(3)-mediated Ca<sup>(2+)</sup> signaling in rat hippocampus astrocytes. *J Neurosci Res.* 2000; 61:409–420. [PubMed: 10931527]

- Karagas MR, Villanueva CM, Nieuwenhuijsen M, Weisel CP, Cantor KP, Kogevinas M. Disinfection byproducts in drinking water and skin cancer? A hypothesis. *Cancer Causes Control*. 2008; 19:547–548. [PubMed: 18219581]
- Kargalioglu Y, McMillan BJ, Minear RA, Plewa MJ. Analysis of the cytotoxicity and mutagenicity of drinking water disinfection by-products in *Salmonella typhimurium*. *Teratogen Carcinogen Mutagen*. 2002; 22:113–128.
- King WD, Marrett LD, Woolcott CG. Case-control study of colon and rectal cancers and chlorination by-products in treated water. *Cancer Epidemiol Biomarkers Prev*. 2000; 9:813–818. [PubMed: 10952098]
- Kogevinas M. Epidemiological approaches in the investigation of environmental causes of cancer: The case of dioxins and water disinfection by-products. *Environ Health*. 2011; 10(Suppl 1):S3. [PubMed: 21489213]
- Komaki, Y.; Pals, J.; Wagner, ED.; Marinas, BJ.; Plewa, MJ. Comparative DNA Damage and Repair Kinetics Study in Mammalian Cells by Chloro-, Bromo-, and Iodoacetic Acid; Environmental Mutagen Society 40th Annual Meeting; St. Louis, MO: Wiley-Blackwell. 2009;
- Krasner SW, Weinberg HS, Richardson SD, Pastor SJ, Chinn R, Scrimanti MJ, Onstad GD, Thruston AD Jr. The occurrence of a new generation of disinfection by-products. *Environ Sci Technol*. 2006; 40:7175–7185. [PubMed: 17180964]
- Kumagai S, Narasaki R, Hasumi K. Glucose-dependent active ATP depletion by koningic acid kills high-glycolytic cells. *Biochem Biophys Res Commun*. 2008; 365:362–368. [PubMed: 17997978]
- Loudon, GM. *Organic Chemistry*. 3rd ed.. Benjamin/Cummings; Redwood, CA: 1995.
- Matthews RT, Ferrante RJ, Jenkins BG, Browne SE, Goetz K, Berger S, Chen IY, Beal MF. Iodoacetate produces striatal excitotoxic lesions. *J Neurochem*. 1997; 69:285–289. [PubMed: 9202321]
- McGuire, MJ.; McLain, JL.; Obolensky, A. Information Collection Rule Data Analysis. American Water Works Association Research Foundation and AWWA; Denver, CO: 2002.
- Muellner MG, Attene-Ramos MS, Hudson ME, Wagner ED, Plewa MJ. Human cell toxicogenomic analysis of bromoacetic acid: A regulated drinking water disinfection by-product. *Environ Mol Mutagen*. 2010; 51:205–214. [PubMed: 19753638]
- Nakajima H, Amano W, Fujita A, Fukuhara A, Azuma YT, Hata F, Inui T, Takeuchi T. The active site cysteine of the proapoptotic protein glyceraldehyde-3-phosphate dehydrogenase is essential in oxidative stress-induced aggregation and cell death. *J Biol Chem*. 2007; 282:26562–26574. [PubMed: 17613523]
- Narotsky MG, Best DS, McDonald A, Godin EA, Hunter ES III, Simmons JE. Pregnancy loss and eye malformations in offspring of F344 rats following gestational exposure to mixtures of regulated trihalomethanes and haloacetic acids. *Reprod Toxicol*. 2011; 31:59–65. [PubMed: 20850520]
- Pals J, Ang J, Wagner ED, Plewa MJ. Biological mechanism for the toxicity of haloacetic acid drinking water disinfection byproducts. *Environ Sci Technol*. 2011; 45:5791–5797. [PubMed: 21671678]
- Peng TI, Jou MJ. Oxidative stress caused by mitochondrial calcium overload. *Ann NY Acad Sci*. 2010; 1201:183–188. [PubMed: 20649555]
- Phillips, HJ. Dye exclusion tests for cell viability. In: Kruse, PF.; Patterson, MJ., editors. *Tissue Culture: Methods and Applications*. Academic Press; New York: 1973. p. 406
- Plewa, MJ.; Wagner, ED. *Mammalian Cell Cytotoxicity and Genotoxicity of Disinfection By-Products*. Water Research Foundation; Denver, CO: 2009. p. 134
- Plewa MJ, Wagner ED, Richardson SD, Thruston AD Jr, Woo YT, McKague AB. Chemical and biological characterization of newly discovered iodoacid drinking water disinfection byproducts. *Environ Sci Technol*. 2004; 38:4713–4722. [PubMed: 15487777]
- Plewa, MJ.; Wagner, ED.; Muellner, MG.; Hsu, KM.; Richardson, SD. Comparative mammalian cell toxicity of N-DBPs and C-DBPs. In: Karanfil, T.; Krasner, SW.; Westerhoff, P.; Xie, Y., editors. *Occurrence, Formation, Health Effects and Control of Disinfection By-Products in Drinking Water*. American Chemical Society; Washington, DC: 2008. p. 36-50.

- Plewa MJ, Simmons JE, Richardson SD, Wagner ED. Mammalian cell cytotoxicity and genotoxicity of the haloacetic acids, a major class of drinking water disinfection by-products. *Environ Mol Mutagen.* 2010; 51:871–878. [PubMed: 20839218]
- Rahman MB, Driscoll T, Cowie C, Armstrong BK. Disinfection by-products in drinking water and colorectal cancer: A meta-analysis. *Int J Epidemiol.* 2010; 39:733–745. [PubMed: 20139236]
- Richard AM, Hunter ES III. Quantitative structure-activity relationships for the developmental toxicity of haloacetic acids in mammalian whole embryo culture. *Teratology.* 1996; 53:352–360. [PubMed: 8910981]
- Richardson, SD. Disinfection by-products: Formation and occurrence in drinking water. In: Nriagu, JO., editor. *Encyclopedia of Environmental Health.* Elsevier; Burlington: 2011. p. 110-136.
- Richardson SD, Plewa MJ, Wagner ED, Schoeny R, DeMarini DM. Occurrence, genotoxicity, and carcinogenicity of regulated and emerging disinfection by-products in drinking water: A review and roadmap for research. *Mutat Res.* 2007; 636:178–242. [PubMed: 17980649]
- Righi E, Bechtold P, Tortorici D, Lauriola P, Calzolari E, Astolfi G, Nieuwenhuijsen MJ, Fantuzzi G, Aggazzotti G. Trihalomethanes, chlorite, chlorate in drinking water and risk of congenital anomalies: A population-based case-control study in Northern Italy. *Environ Res.* 2012; 116:66–73. [PubMed: 22578809]
- Rundell MS, Wagner ED, Plewa MJ. The comet assay: Genotoxic damage or nuclear fragmentation? *Environ Mol Mutagen.* 2003; 42:61–67. [PubMed: 12929117]
- Sakai A, Shimizu H, Kono K, Furuya E. Monochloroacetic acid inhibits liver gluconeogenesis by inactivating glyceraldehyde-3-phosphate dehydrogenase. *Chem Res Toxicol.* 2005; 18:277–282. [PubMed: 15720133]
- Schlisser AE, Yan J, Hales BF. Teratogen-induced oxidative stress targets glyceraldehyde-3-phosphate dehydrogenase in the organo-genesis stage mouse embryo. *Toxicol Sci.* 2010; 118:686–695. [PubMed: 20889679]
- Smith HS. In vitro properties of epithelial cell lines established from human carcinomas and nonmalignant tissue. *J Natl Cancer Inst.* 1979; 62:225–230. [PubMed: 283258]
- Tice RR, Agurell E, Anderson D, Burlinson B, Hartmann A, Kobayashi H, Miyamae Y, Rojas E, Ryu JC, Sasaki YF. Single cell gel/comet assay: Guidelines for in vitro and in vivo genetic toxicology testing. *Environ Mol Mutagen.* 2000; 35:206–221. [PubMed: 10737956]
- Tristan C, Shahani N, Sedlak TW, Sawa A. The diverse functions of GAPDH: Views from different subcellular compartments. *Cell Signal.* 2011; 23:317–323. [PubMed: 20727968]
- U.S. Environmental Protection Agency. Quantification of Cancer Risk from Exposure of Chlorinated Drinking Water. Office of Water, Office of Science and Technology, Health and Ecological Criteria Division; Washington, DC: 1998.
- U.S. Environmental Protection Agency. National primary drinking water regulations: Stage 2 disinfectants and disinfection byproducts rule. *Fed Reg.* 2006; 71:387–493.
- Villanueva CM, Cantor KP, Cordier S, Jaakkola JJ, King WD, Lynch CF, Porru S, Kogevinas M. Disinfection byproducts and bladder cancer: A pooled analysis. *Epidemiology.* 2004; 15:357–367. [PubMed: 15097021]
- Villanueva CM, Cantor KP, Grimalt JO, Malats N, Silverman D, Tardon A, Garcia-Closas R, Serra C, Carrato A, Castano-Vinyals G, Marcos R, Rothman N, Real FX, Dosemeci M, Kogevinas M. Bladder cancer and exposure to water disinfection byproducts through ingestion, bathing, showering, and swimming in pools. *Am J Epidemiol.* 2007; 165:148–156. [PubMed: 17079692]
- Wagner, ED.; Plewa, MJ. Microplate-based comet assay. In: Dhawan, A.; Anderson, D., editors. *The Comet Assay in Toxicology.* Royal Society of Chemistry; London: 2009. p. 79-97.
- Wagner ED, Rayburn AL, Anderson D, Plewa MJ. Analysis of mutagens with single cell gel electrophoresis, flow cytometry, and forward mutation assays in an isolated clone of Chinese hamster ovary cells. *Environ Mol Mutagen.* 1998; 32:360–368. [PubMed: 9882011]
- Wei X, Wang S, Zheng W, Wang X, Liu X, Jiang S, He G, Zheng Y, Qu W. Drinking water disinfection byproduct iodoacetic acid induces tumorigenic transformation of NIH3T3 cells. *Environ Sci Technol.* 47:5913–5920. [PubMed: 23641915]

- Zhang SH, Miao DY, Liu AL, Zhang L, Wei W, Xie H, Lu WQ. Assessment of the cytotoxicity and genotoxicity of haloacetic acids using microplate-based cytotoxicity test and CHO/HGPRT gene mutation assay. *Mutat Res.* 2010; 703:174–179. [PubMed: 20801231]
- Zhang, X.; Echigo, S.; Minear, RA.; Plewa, MJ. Characterization and comparison of disinfection by-products of four major disinfectants. In: Barrett, SE.; Krasner, SW.; Amy, GL., editors. *Natural Organic Matter and Disinfection By-Products: Characterization and Control in Drinking Water.* American Chemical Society; Washington, DC: 2000. p. 299-314.

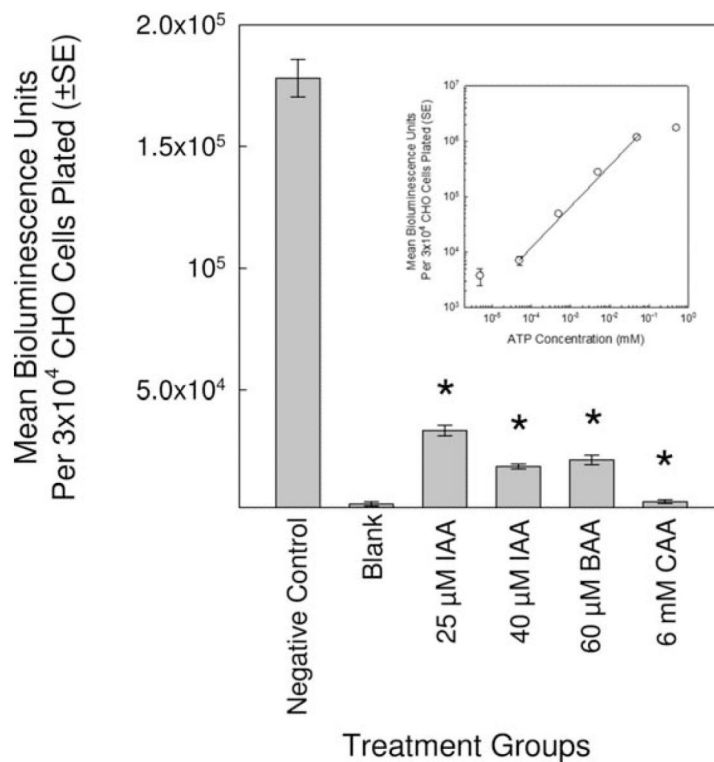


**Fig. 1.** Impact of monoHAA exposure on the cellular ATP levels as measured using relative bioluminescence units. The \* indicates a significant difference from the negative control. The insert is a ATP standard curve.

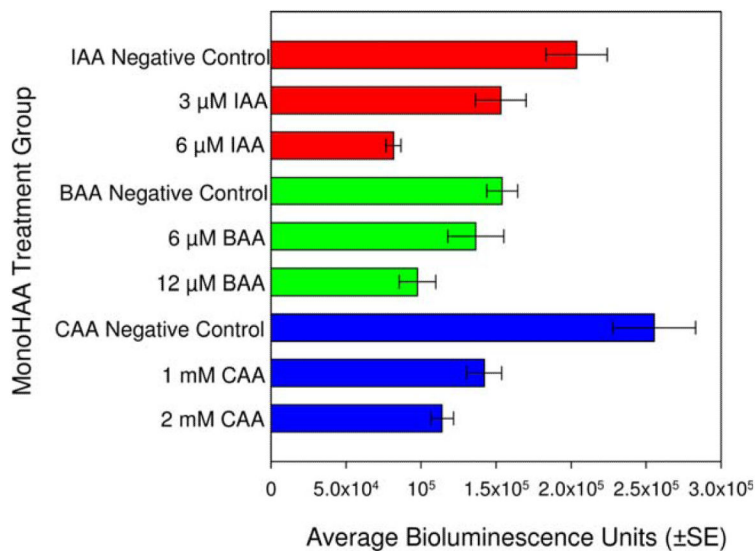


**Fig. 2.** Reduction of ATP levels measured as bioluminescence units in CHO cells after exposure to monoHAAs. All monoHAA treatments induced a significant reduction in ATP levels as compared to the concurrent negative controls. [Color figure can be viewed in the online issue, which is available at [wileyonlinelibrary.com](http://wileyonlinelibrary.com).]



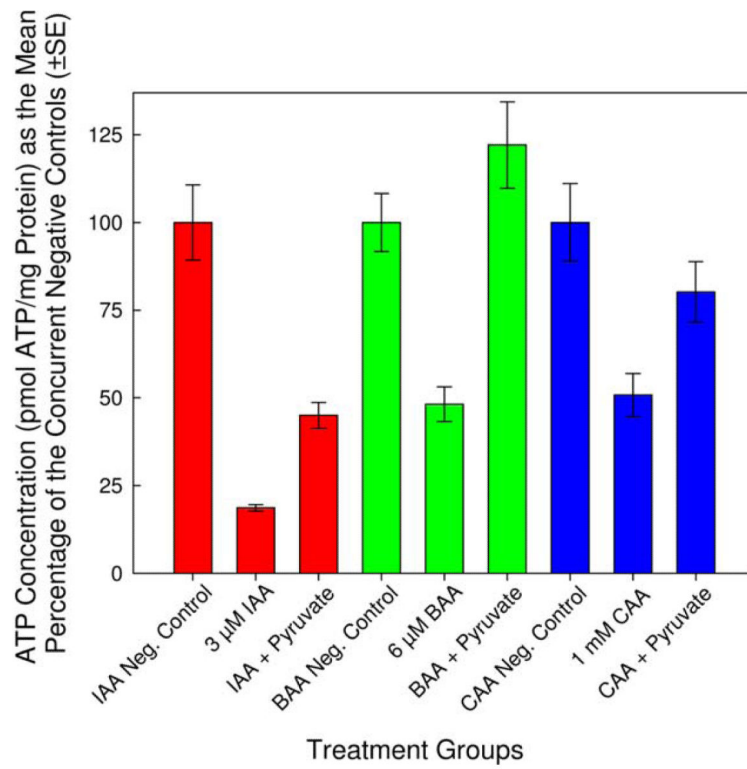


**Fig. 3.** Recovery of ATP levels in monoHAA-treated cells after pyruvate supplementation. [Color figure can be viewed in the online issue, which is available at [wileyonlinelibrary.com](http://wileyonlinelibrary.com).]

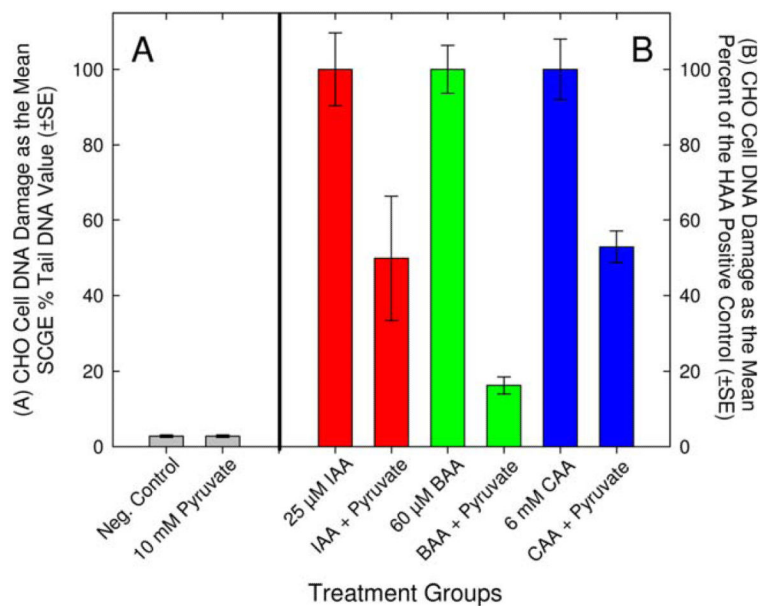


**Fig. 4.** Reduction of monoHAA-induced genomic DNA damage by pyruvate supplementation. **(A)** The SCGE % tail DNA values for the negative control and for 10 mM pyruvate. **(B)** MonoHAA-induced DNA damage normalized as 100% for the positive controls and the reduction in DNA damage with pyruvate supplementation. [Color figure can be viewed in the online issue, which is available at [wileyonlinelibrary.com](http://wileyonlinelibrary.com).]

**TABLE I**  
**Monohaloacetic Acid Characteristics, Sources, and Purities**

HAA <sup>a</sup>	CASN	MW (g/mol)	C-X <sup>b</sup>	Bond length (Å) <sup>c</sup>	Dissociation energy (kcal/mol) <sup>d</sup>	Source	Purity
IAA	64-69-7	185.95	C-I	2.14	57.4	Sigma- Aldrich	>99%
BAA	79-08-3	138.95	C-Br	1.93	65.9	Fluka	>99%
CAA	79-11-8	94.50	C-Cl	1.77	78.5	Fluka	>99%

<sup>a</sup>HAA, haloacetic acids; IAA, iodoacetic acid; BAA, bromoacetic acid; CAA, chloroacetic acid.

<sup>b</sup>α-Carbon-halogen bond.

<sup>c</sup>C-X bond length summarized from [Loudon, 1995].

<sup>d</sup>C-X bond dissociation energy summarized from [Loudon, 1995].

**TABLE II**  
**Effect of the HAAs on ATP Levels in CHO Cells With and Without Pyruvate**  
**Supplementation**

HAA group	Treatment conditions	pmol ATP/mg protein mean value $\pm$ SE	% Reduction per pmol HAA
IAA	Negative control (IAA)	29788 $\pm$ 3197	NA
	10 mM pyruvate	29476 $\pm$ 3575	NA
	3 $\mu$ M IAA	5557 $\pm$ 274	0.54229
	3 $\mu$ M IAA + pyruvate	13411 $\pm$ 1105	NA
BAA	Negative control (BAA)	18225 $\pm$ 1503	NA
	10 mM pyruvate	29297 $\pm$ 2782	NA
	6 $\mu$ M BAA	8786 $\pm$ 897	0.15136
	6 $\mu$ M BAA + pyruvate	24338 $\pm$ 2487	NA
CAA	Negative control (CAA)	6814 $\pm$ 755	NA
	10 mM pyruvate	23464 $\pm$ 2278	NA
	1 mM CAA	3463 $\pm$ 419	0.00098
	1 mM CAA + pyruvate	5465 $\pm$ 589	NA

NA, not applicable.

**TABLE III**  
**Pearson Product Moment Correlation Analyses of HAA Physicochemical Parameters and the Percent Reduction of Cellular ATP per pmol HAA in CHO Cells**

Physicochemical parameters	ELUMO (r) <sup>a</sup>	$\alpha$ C-X bond length (r) <sup>b</sup>	$\alpha$ C-X dissociation energy (r) <sup>b</sup>	Relative alkylation potential (S <sub>N</sub> 2) (r) <sup>b</sup>
ATP % reduction per pmol HAA <sup>c</sup>	-0.986	0.985	-0.935	0.999
ELUMO		-1.000	0.981	-0.980
C-X bond length			-0.982	0.979
C-X dissociation energy				-0.922

<sup>a</sup> Calculated ELUMO (energy of the lowest unoccupied molecular orbital) summarized from [Richard and Hunter, 1996].

<sup>b</sup> Summarized from [Loudon, 1995].

<sup>c</sup> Calculated from data presented in this study.

**TABLE IV**  
**Pearson Product Moment Correlation Analyses of HAA Toxicological Parameters and the Percent Reduction of Cellular ATP per pmol HAA in CHO Cells**

HAA toxicological parameters	CHO cell cytotoxic index ( <i>r</i> )	CHO cell genotoxic index ( <i>r</i> )	FHs cell genotoxic index ( <i>r</i> )	Salmonella cytotoxic index ( <i>r</i> )	Salmonella mutagenic potency ( <i>r</i> )	CHO cell mutagenicity index ( <i>r</i> )	Mouse teratogenicity ( <i>r</i> )	GAPDH inhibition ( <i>r</i> )
ATP % reduction per pmol HAA <sup>a</sup>	1.00	0.968	0.992	0.991	0.993	0.965	0.999	-0.986
CHO cell cytotoxic index <sup>b</sup>		0.976	0.996	0.995	0.996	0.956	0.998	-0.990
CHO cell genotoxic index <sup>c</sup>			0.992	0.993	0.991	0.868	0.959	-0.997
FHs cell genotoxic index <sup>c</sup>				1.00	1.00	0.925	0.987	-0.999
Salmonella cytotoxic index <sup>d</sup>					1.00	0.921	0.986	-0.999
Salmonella mutagenic potency <sup>d</sup>						0.926	0.988	-0.999
CHO cell mutagenicity index <sup>e</sup>							0.974	-0.906
Mouse teratogenicity <sup>f</sup>								-0.979
GAPDH inhibition kinetics <sup>g</sup>								1.00

<sup>a</sup>Calculated from data presented in this study.

<sup>b</sup>Derived as the reciprocal of the LC<sub>50</sub> concentration (× constant to generate whole numbers), data from [Plewa et al., 2010].

<sup>c</sup>Derived as the reciprocal of the SCGE genotoxic potency value (× constant to generate whole numbers), data from [Plewa et al., 2010; Pals et al., 2011].

<sup>d</sup>Data from [Kargalioglu et al., 2002; Plewa et al., 2004].

<sup>e</sup>Data from [Zhang et al., 2010].

<sup>f</sup>Data from [Hunter et al., 1996].

<sup>g</sup>The average rate of GAPDH inhibition per μM monoHAA concentration derived from the slope of the inhibition curves for each monoHAA [Pals et al., 2011].



**TABLE V**  
**Induction of Genomic SCGE DNA Damage in CHO Cells by HAAs With and Without Pyruvate Supplementation**

Treatment groups	Number of microgels	Mean SCGE % tail DNA value ( $\pm$ SE)	ANOVA test statistic $F_{7,81} = 74.4$ ; $P = 0.001$
Negative control (a)	18	2.80 $\pm$ 1.33	a
10 mM pyruvate control (b)	10	2.79 $\pm$ 1.03	a vs. b ( $P = 0.998$ )
25 $\mu$ M IAA (c)	12	21.5 $\pm$ 2.07	c vs. a ( $P = 0.001$ )
25 $\mu$ M IAA +10mM pyruvate (d)	10	10.6 $\pm$ 3.50	d vs. c ( $P = 0.001$ )
60 $\mu$ M BAA (e)	10	49.8 $\pm$ 3.17	e vs. a ( $P = 0.001$ )
60 $\mu$ M BAA + 10 mM pyruvate (f)	10	8.09 $\pm$ 1.13	f vs. e ( $P = 0.001$ )
6mM CAA (g)	8	47.2 $\pm$ 3.79	g vs. a ( $P = 0.001$ )
6 mM CAA + 10 mM pyruvate (h)	11	24.9 $\pm$ 1.98	h vs.g ( $P = 0.001$ )